NAVAL POSTGRADUATE SCHOOL

MONTEREY, CALIFORNIA

THESIS

DIURNAL SEA BREEZE EFFECTS ON NEARSHORE TEMPERATURE VARIABILITY IN SOUTHERN MONTEREY BAY

by

Aaron M. Morrone

December 2017

Thesis Advisor:	Jamie MacMahan
Second Reader:	Ed Thornton

Approved for public release. Distribution is unlimited.

THIS PAGE INTENTIONALLY LEFT BLANK

REPORT DOCUMENTATION PAGE	*Form Approved OMB No. 0704–0188*

1. AGENCY USE ONLY ***(Leave blank)***	**2. REPORT DATE** December 2017	**3. REPORT TYPE AND DATES COVERED** Master's thesis

4. TITLE AND SUBTITLE DIURNAL SEA BREEZE EFFECTS ON NEARSHORE TEMPERATURE VARIABILITY IN SOUTHERN MONTEREY BAY	**5. FUNDING NUMBERS**
6. AUTHOR(S) Aaron M. Morrone	
7. PERFORMING ORGANIZATION NAME(S) AND ADDRESS(ES) Naval Postgraduate School, Monterey, CA 93943-5000	**8. PERFORMING ORGANIZATION REPORT NUMBER**
9. SPONSORING /MONITORING AGENCY NAME(S) AND ADDRESS(ES) N/A	**10. SPONSORING / MONITORING AGENCY REPORT NUMBER**

11. SUPPLEMENTARY NOTES The views expressed in this thesis are those of the author and do not reflect the official policy or position of the Department of Defense or the U.S. Government. IRB number ____N/A____.

12a. DISTRIBUTION / AVAILABILITY STATEMENT Approved for public release. Distribution is unlimited.	**12b. DISTRIBUTION CODE**

13. ABSTRACT (maximum 200 words)

Forty-five days of co-located temperature and velocity profiles were obtained from two cross-shore arrays spanning between water depths of 5m and 10m (100m in the cross-shore and 150m in the alongshore) off Del Monte Beach, CA in southern Monterey Bay. A canonical day, based on local time, is chosen due to the occurrence of diurnal sea breeze that is commonly observed in the bay. Under relatively weak cross-shore wind- (<0.03 Pa) and wave-forcing (H_{rms}<0.5m), afternoon temperatures warm ~1.5°C in 5m and 10m water depths. The cross-shore heat flux (CHF) reaches a maximum of $4x10^5$W/m in the afternoon in 10m water depth, while the CHF remains at zero throughout the day in 5m water depth. The relative difference in water temperature between 5m and 10m water depths results in ~0.5°C increase at 5m and corresponds with the trends in CHF. During night, under minimal wind forcing, the CHF at 10m water depth decreases to near zero and the water temperature increases by ~0.3°C compared to 5m water depth. The location of the zero CHF represents a canonical day surface transport barrier where material accumulates, which described herein is heat.

14. SUBJECT TERMS nearshore, flux, temperature variability, cross-shore heat flux, surface heat flux, diurnal, sea breeze, boundary, warming	**15. NUMBER OF PAGES** 37
	16. PRICE CODE

17. SECURITY CLASSIFICATION OF REPORT	**18. SECURITY CLASSIFICATION OF THIS PAGE**	**19. SECURITY CLASSIFICATION OF ABSTRACT**	**20. LIMITATION OF ABSTRACT**
Unclassified	Unclassified	Unclassified	UU

NSN 7540–01-280-5500 — Standard Form 298 (Rev. 2–89) Prescribed by ANSI Std. 239–18

THIS PAGE INTENTIONALLY LEFT BLANK

Approved for public release. Distribution is unlimited.

DIURNAL SEA BREEZE EFFECTS ON NEARSHORE TEMPERATURE VARIABILITY IN SOUTHERN MONTEREY BAY

Aaron M. Morrone
Lieutenant Commander, United States Navy
B.S., United States Naval Academy, 2007

Submitted in partial fulfillment of the
requirements for the degree of

MASTER OF SCIENCE IN METEOROLOGY AND PHYSICAL OCEANOGRAPHY

from the

NAVAL POSTGRADUATE SCHOOL
December 2017

Approved by: Jamie MacMahan
Thesis Advisor

Ed Thornton
Second Reader

Peter Chu
Chair, Department of Oceanography

THIS PAGE INTENTIONALLY LEFT BLANK

ABSTRACT

Forty-five days of co-located temperature and velocity profiles were obtained from two cross-shore arrays spanning between water depths of 5m and 10m (100m in the cross-shore and 150m in the alongshore) off Del Monte Beach, CA, in southern Monterey Bay. A canonical day, based on local time, is chosen due to the occurrence of diurnal sea breeze that is commonly observed in the bay. Under relatively weak cross-shore wind- (<0.03 Pa) and wave-forcing (H_{rms}<0.5m), afternoon temperatures warm ~1.5°C in 5m and 10m water depths. The cross-shore heat flux (CHF) reaches a maximum of $4x10^5$W/m in the afternoon in 10m water depth, while the CHF remains at zero throughout the day in 5m water depth. The relative difference in water temperature between 5m and 10m water depths results in ~0.5°C increase at 5m and corresponds with the trends in CHF. During night, under minimal wind forcing, the CHF at 10m water depth decreases to near zero and the water temperature increases by ~0.3°C compared to 5m water depth. The location of the zero CHF represents a canonical day surface transport barrier where material accumulates, which described herein is heat.

THIS PAGE INTENTIONALLY LEFT BLANK

TABLE OF CONTENTS

I. INTRODUCTION **1**

II. FIELD EXPERIMENT AND METHODS **3**

III. RESULT—CANONICAL DAY **7**

IV. DISCUSSION **11**

V. CONCLUSION **15**

LIST OF REFERENCES **17**

INITIAL DISTRIBUTION LIST **21**

THIS PAGE INTENTIONALLY LEFT BLANK

LIST OF FIGURES

Figure 1. Aerial image of Del Monte Beach in Southern Monterey Bay where cross-shore heat flux experiment was conducted just seaward of the surf zone. 4

Figure 2. Hourly averaged canonical day conditions. 7

Figure 3. Canonical day water temperatures over the vertical. 8

Figure 4. CHF at 10-meters water depth (solid black line) and 5-meters water depth (dashed black line). Shading indicates 95% confidence intervals about the mean including both cross-shore arrays. 9

THIS PAGE INTENTIONALLY LEFT BLANK

LIST OF ACRONYMS AND ABBREVIATIONS

$\Delta T_{5m\text{-}10m}$	upper 5m of the 10m water column subtracted from the 5m water column
τ^{sx}	cross-shore wind stress
τ^{sy}	alongshore wind stress
ADCP	acoustic Doppler current profiler
AHF	alongshore heat flux
CHF	cross-shore heat flux
H_L	latent heat
H_{LW}	long wave radiation
H_S	sensible heat
H_{SW}	shortwave radiation
SHF	surface heat flux
T-strings	thermistor strings

THIS PAGE INTENTIONALLY LEFT BLANK

ACKNOWLEDGMENTS

I would like to thank my advisor, Professor Jamie MacMahan, for his tireless devotion to guide [push], and help me through to the finish. His knowledge, patience, passion for science, and caring attitude made it an amazing learning experience. I am thankful to have worked alongside him during this process and to have gained a lifetime of science memories I will not forget ("You have the data; the paper writes itself!").

In addition, I would like to thank Tucker Freismuth, who was never too busy to help me or act as my sounding board. His understanding of science and MATLAB skills are second to none. I have no doubt in your future Ph.D. completion.

I also am grateful to Matt Gough, a.k.a. Bob Ross, for your input and editing that turned my sentences into a scientific paper. I also would like to thank Ed Thornton, a legend in the nearshore field, for being my second reader and providing clear and concise input. Finally, I want to acknowledge my classmates, who were always there to share laughs along the way. Be safe out in the fleet!

And last, but certainly not least, I would like to thank my amazing wife, Alison, for her dedication, understanding, and unconditional love as she continues to walk by my side through this journey we started here in Monterey. She offered gentle reminders when I needed to focus on school and made sure I was taken care of. She is the epitome of selflessness. This thesis is as much hers as it is mine.

THIS PAGE INTENTIONALLY LEFT BLANK

I. INTRODUCTION

The understanding of the cross-shore exchange of material across and into the inner shelf as well as the exchange into and out of the surf zone has gained considerable attention. Great strides have been made in describing the forcing mechanisms responsible for the observed circulation and corresponding exchange (Lentz and Fewings 2012). The inner shelf is dynamically defined as *seaward* of the surf zone, where depth-limited wave breaking occurs, and *shoreward* of the midshelf, where the surface mixed layer and bottom boundary layer converge in the water column (Lentz and Fewings 2012). The cross-shore transport as described over the vertical for the inner shelf is concomitantly forced by wind and waves (Tilburg 2003; Lentz et al. 2008; Fewings et al. 2008; Lentz and Fewings 2012) and modified by vertical and horizontal stratification (Horowitz and Lentz 2014). The cross-shore exchange into the inner shelf that originates from the surf zone has been primarily attributed to both stationary and transient rip currents that can extend 2–4 surf zone widths from the shoreline (Clark et al. 2012; Feddersen 2014; Brown et al. 2015; Hally-Rosendahl et al. 2015; Kumar and Feddersen 2017a; Kumar and Feddersen 2017b). In addition, internal waves can also transport material into and across the inner shelf (Pineda 1994; Noble et al. 2009; Walter et al. 2012; Walter et al. 2017) and ultimately into the surf zone (Sinnett and Feddersen 2014).

The current understanding of inner shelf cross-shore transport processes comes from many field experiments ranging from multi-year, single-location measurements of the velocity profiles (Fewings et al. 2008; Lentz et al. 2008; Hendrickson and MacMahan 2009) to shorter O(0-2 months) experiments with multi-location moorings (Hally-Rosendahl et al. 2015; Reniers et al. 2009). Direct approaches for accounting for material transport have included the deployment and mapping of fluorescent dye (Grant et al. 2005; Clarke et al. 2007; Clark et al. 2014; Hally-Rosendahl et al. 2015) to the tracking of GPS-equipped surface drifters (Spydell et al. 2007; Brown et al. 2009; Brown et al. 2015; Roth et al. 2016; Spydell 2016) to estimating heat fluxes and gradients in heat fluxes owing to the natural temporal and spatial variability of ocean water temperature

(Lentz 1987; Send et al. 1987; Dever and Lentz 1994; Austin 1999; Fewings and Lentz 2011; Suanda et al. 2011; Sinnett and Feddersen 2014; Walter et al. 2017).

The inner shelf cross-shore exchange has been described for the subtidal (>33hrs) variability (Fewings et al. 2008; Fewings and Lentz 2011) and for the supertidal (<33hrs) variability associated with diurnal, sea breeze driven events (Kaplan et al. 2003; Suanda et al. 2011; Walter et al. 2017). Many of the inner shelf experiments extend to as shallow as 10m water depth (Lentz et al. 2008; Fewings et al. 2008; Suanda et al. 2011; Walter et al. 2017). Only a few experiments have focused on the cross-shore in the shallower water depths of the inner shelf extending from 10m water depth to the edge of the surf zone (Brown et al. 2015; Hally-Rosendahl et al. 2015). These experiments emphasize the surf zone contribution to the inner shelf.

Here, the canonical trends are determined from the interrelationship between the water column temperature, the cross-shore heat flux, gradients in the cross-shore heat flux, and diurnal onshore wind forcing *with emphasis on the inner shelf transport from 10m to 5m water depth (edge of the surf zone)* in southern Monterey Bay, CA. It is hypothesized that surface waters in shallow water will warm in the late afternoon, similar to the findings of Kaplan et al. (2003) for water depths as shallow as 12m and in a shallow-water lagoon by Herdman et al. (2015). This work also builds on the effort by Hendrickson and MacMahan (2009), who found that diurnal afternoon, onshore sea breeze winds induce onshore flows at the surface and offshore flows at depth in 13m water depth in central Monterey Bay, CA. In the Monterey Bay, the land breeze is minimal and only the sea breeze is the dominant diurnal signal. The diurnal transport patterns observed by Hendrickson and MacMahan (2009) are consistent with subtidal wind- and wave-forced cross-shore response described by Fewings et al. (2008). The new observations presented here provide additional insights into diurnal warming and cooling trends just seaward of the surf zone.

II. FIELD EXPERIMENT AND METHODS

Two cross-shore arrays consisting of bottom-mounted acoustic Doppler current profilers (ADCPs) co-located with temperature strings were deployed between 5 and 10m water depths off Del Monte Beach, CA from 3 June 2016 to 18 July 2016 (yeardays 155–200). The beach is located in the southern corner of Monterey Bay and is oriented east-west at an angle of 58 degrees from due north (Figure 1). Each array is designed to estimate the cross-shore heat flux from 10m to the nominal edge of the surf zone (~5m). Two cross-shore arrays were deployed to account for the spatial heterogeneity of cross-shore flows associated with rip currents on the inner shelf (Brown et al. 2015). The cross-shore arrays were separated by 150m in the alongshore, which is approximately 1.5 alongshore rip current spacing (MacMahan et al. 2005; MacMahan et al. 2006). The spacing should allow for simultaneous measurement of both onshore and offshore directed rip currents, accounting for the potential alongshore rip channel migration (Orzech et al. 2010) that may occur over the 45-day experiment.

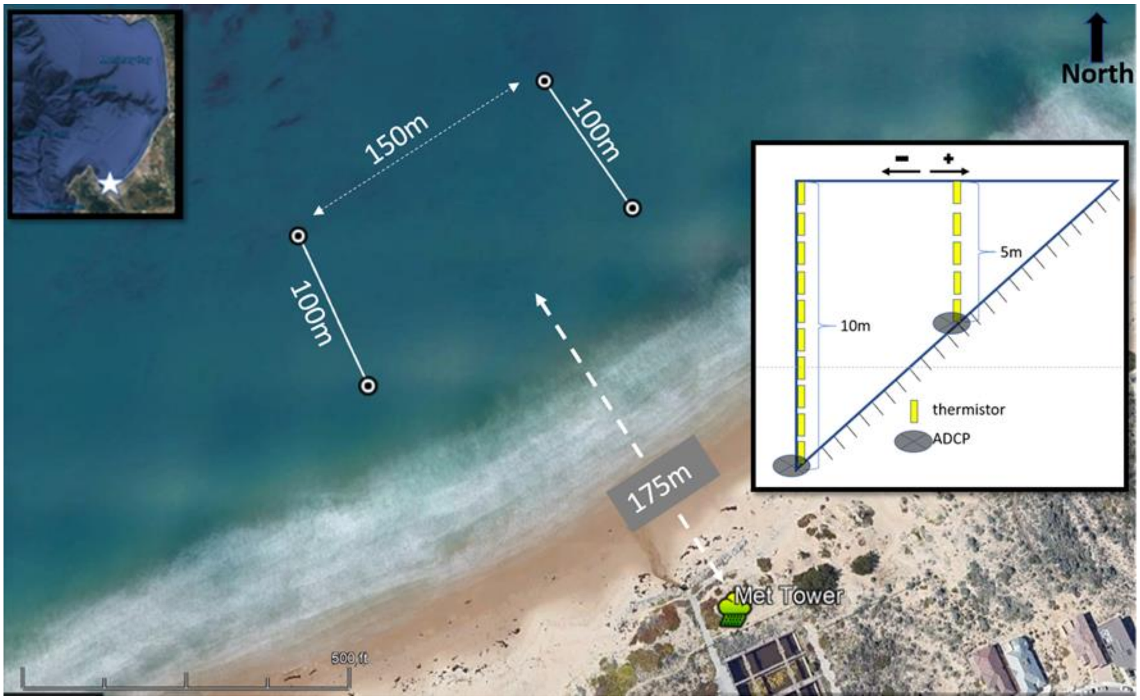

The location of the two cross-shore arrays is indicated by the white line. Located 175m onshore is the met tower. Data acquisition lasted 2.5 months. The insert on the right represents a 2-D cross-shore slice of the array showing the location of the thermistors and ADCP in 10 m and 5 m isobath. Positive velocities are shoreward.

Figure 1. Aerial image of Del Monte Beach in Southern Monterey Bay where cross-shore heat flux experiment was conducted just seaward of the surf zone.

Bottom-mounted, upward facing 2MHz, ADCPs were mounted on sea-spiders approximately 0.5m off the sea floor. The ADCPs measured horizontal current velocities at 35cm vertical bins with a 2.5-minute block average sample rate. Owing to the 2.5-minute sample rate, individual, self-logging pressure sensors were deployed on each sea spider, sampling at 1 Hz. Wave height, H_{rms}, was estimated by applying linear wave theory to the pressure data from the self-loggers. Co-located with the ADCPs, were temperature strings (T-strings) composed of individual, self-logging temperature sensors spaced at 1m increments in the vertical with 0.002°C accuracy sampling at 1 Hz. Tilt sensors were placed mid-depth on T-strings for estimating blow over, which never occurred for these moorings. ADCP velocities near the sea surface were removed. All velocities were rotated by 58 degrees to a local shoreline orientation, where u and v components represent the cross-shore and alongshore flows. The subscripts 10m and 5m will denote the mooring water depth.

A 10m meteorological tower is deployed on a 25m high dune located 175m shoreward from the 5m water depth mooring measuring wind speed and direction, upward and downward long- (H_{LW}) and short-wave (H_{SW}) radiation, air temperature, and relative humidity sampling at 2 minutes (Figure 1). Wind stress is computed following Large and Pond (1982). The wind stress is rotated into a local shoreline orientation. The peak winds correspond to a wind stress of 0.04Pa and the mean wind corresponds to a wind stress of 0.01Pa. The surface heat flux (SHF) is estimated from direct measurements of H_{SW} and H_{LW} that are added to estimates of sensible and latent heat fluxes following the bulk formula by Pawlowicz et al. (2001).

All data are hourly averaged and represented as a canonical day. A canonical day represents an ensemble average (multiple days) of processes that repeat diurnally to increase statistical confidence about the behavior. Canonical day analyses are ideal for capturing trends in wind forcing due to the afternoon sea breeze (Herdman et al. 2015; Lamas et al. 2017; Molina et al. 2014), as commonly observed in Monterey Bay (Hendrickson and MacMahan 2009; Suanda et al. 2011). The observations from the two cross-shore arrays are averaged in the alongshore to account for spatial heterogeneity and to further increase statistical confidence.

The cross-shore heating and cooling of the water column is determined from a canonical day heat flux balance. For a two-dimensional system, assuming that the alongshore gradient in temperature (referred to as AHF) and velocity is zero, the conservation of heat can be written as:

$$\rho\, C_p\left(\frac{\partial T}{\partial t}+\frac{\partial (uT)}{\partial x}+\frac{\partial (wT)}{\partial z}\right)=\frac{\partial q}{\partial z} \tag{1}$$

where ρ is the density of water, C_p is the specific heat of water, T is temperature, q is the total of all the heat sources and represents the SHF herein, u represents the cross-shore velocity, w represents the vertical velocity, and z is position from the bottom upwards (Herdman et al. 2015). The second and third terms on the right-hand side of the equation are the cross-shore and vertical divergence of heat flux. uT represents the cross-shore heat flux (CHF). The vertical divergence of heat flux can be eliminated with the assumption that the vertical velocity is zero at the surface and bottom (Herdman et al. 2015). The equation then reduces to:

$$\rho C_p\left(\frac{\partial T}{\partial t}+\frac{\partial (uT)}{\partial x}\right)=\frac{\partial q}{\partial z} \tag{2}$$

The canonical depth-integrated CHF at 10m and 5m is obtained with the following procedure. The temperature obtained by each thermistor is vertically interpolated onto the ADCP bin depths. The hourly perturbations of temperature and velocity are computed by subtracting the depth-averaged temperature and velocity for the entire experiment from the hourly temperature and velocity at each depth. The hourly perturbations of temperature are multiplied by hourly perturbations of velocity, which represent fluxes associated with the baroclinic signal or two-layer flow. A CHF is described by the depth-integrated flux that is canonically-averaged.

III. RESULT—CANONICAL DAY

The canonical day cross- (τ^{sx}) and alongshore (τ^{sy}) wind stresses exhibit a 95% statistically significant pattern. τ^{sx} increases from 0800 to a maximum of 0.03Pa at 1200 and decreases to zero at 2000 (Figure 2a). There is a diurnal wind stress rotation from cross-shore to alongshore. τ^{sy} increases from 1000 to a maximum of 0.03Pa at 1500 and decreases to near zero at 2400 (Figure 2a). Since $\tau^{sx} \leq 0.03$Pa, the inner shelf region is considered weakly forced by winds (Fewings et al. 2008). There is no 95% statistically significant canonical variability for H_{rms}, and can be described at ~0.5 m (Figure 2b). The canonical SHF pattern is statistically significant at the 95% confidence interval. SHF begins increasing at 0700 to a maximum of 800W/m^2 at 1300 and decreases to near zero at 1800 where it remains until the following morning at 0700 (Figure 2c). When SHF is negative, it cools the water surface, whereas positive values warm the water surface. There is a relative inequality of the heating and cooling, though both scenarios are ~12 hours in duration.

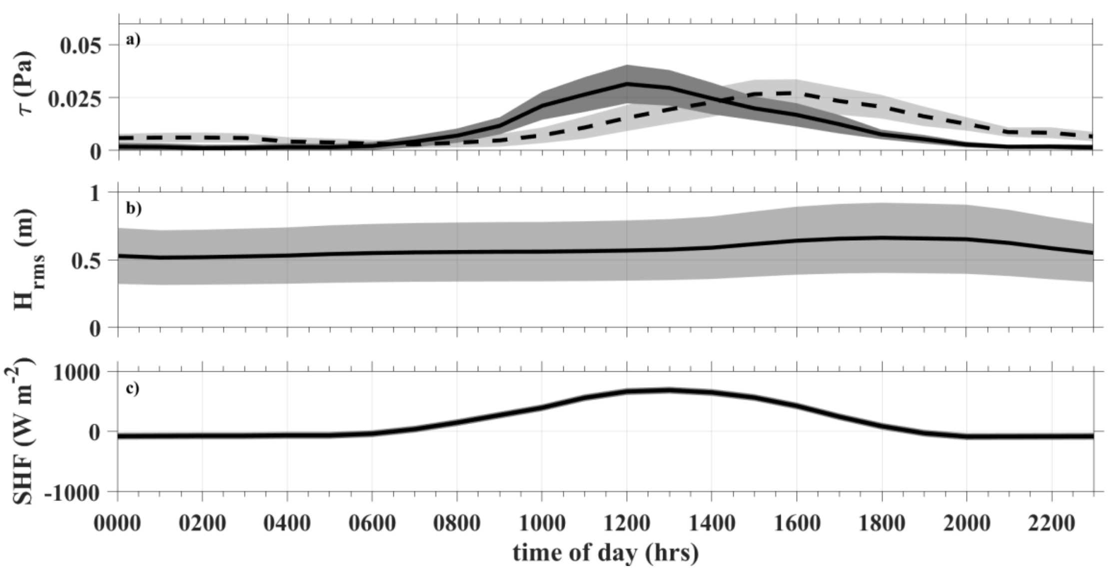

(a) Wind stress broken into u (cross-shore) shown as solid black line, and v (alongshore) shown as dashed black line, components; (b) wave height at 5-meter water depth; (c) surface heat flux. Shading indicates 95% confidence intervals about the mean.

Figure 2. Hourly averaged canonical day conditions.

The canonical day temperatures over the vertical at 10m (T_{10m}) and 5m (T_{5m}) exhibit a range between 12°C and 16°C with nearshore warming starting at 0800 with a maximum surface temperature near 1700 (Figures 3a and 3b). As the surface waters warm, the warm layer extends deeper into the water column by a couple of meters. Near 1700, the surface waters begin to cool until 0800 the next morning (Figures 3a and 3b).

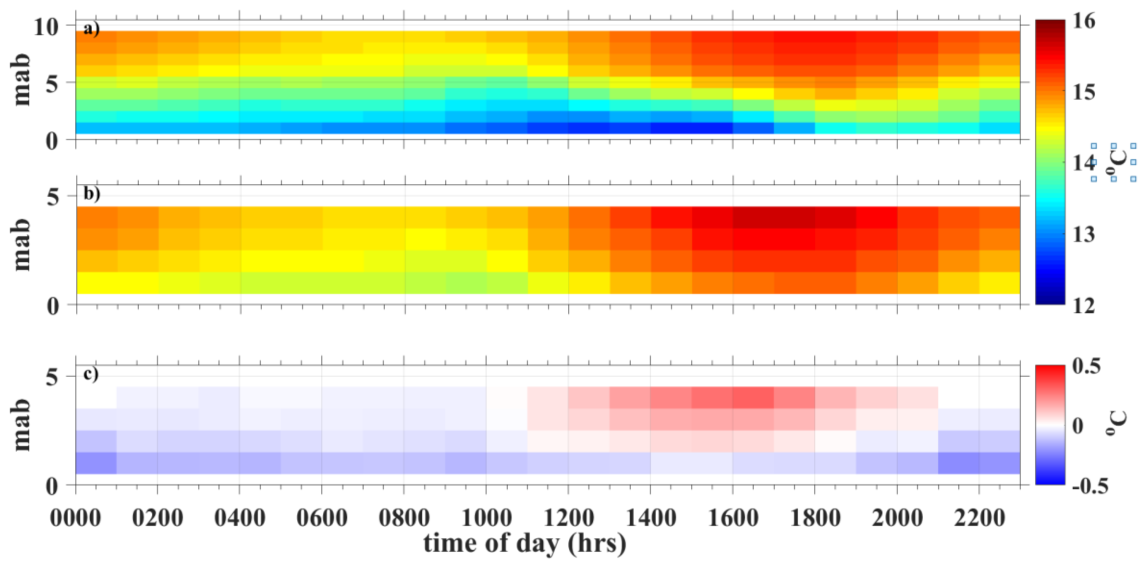

a) 10-meter water depth; b) 5-meter water depth averaged over the two cross-shore arrays; c) upper half of 10-meter water depth subtracted from 5-meter water depth (ΔT_{5m-10m}). In all plots, red indicates warmer and blue indicates cooler temperatures.

Figure 3. Canonical day water temperatures over the vertical.

The canonical CHF_{10m} (solid line, Figure 4) at the 95% significance level, statistically varies for the 10m mooring. It increases at 0800, peaks to $4x10^5$W/m at 1600, then decreases to a background level of $1x10^5$W/m at 2100. CHF_{5m} (dotted line, Figure 4) does not statistically differ from zero at the 95% significance level. This states that there is a canonical CHF_{10m} depth that varies, and reduces to zero in 5m, which is only separated by 100m in the cross-shore.

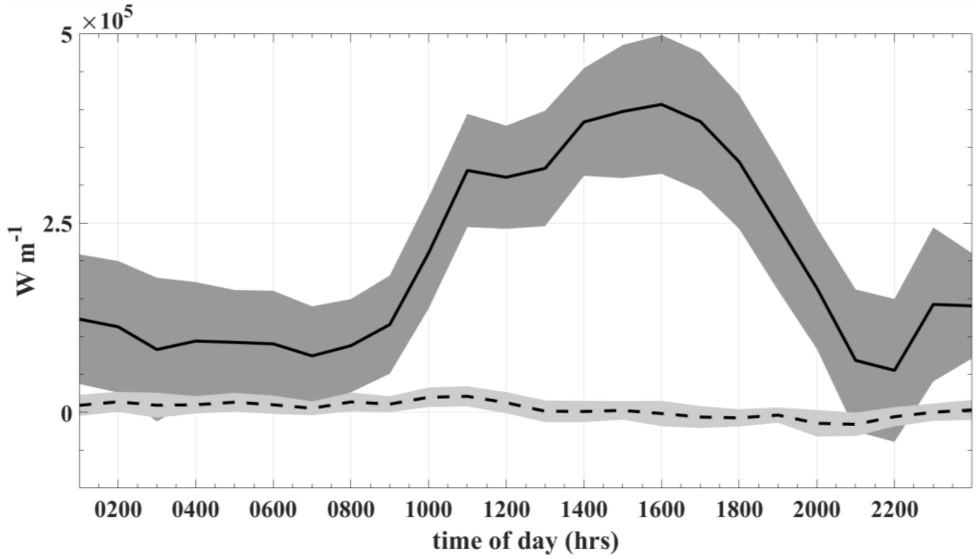

Figure 4. CHF at 10-meters water depth (solid black line) and 5-meters water depth (dashed black line). Shading indicates 95% confidence intervals about the mean including both cross-shore arrays.

THIS PAGE INTENTIONALLY LEFT BLANK

IV. DISCUSSION

In the canonical averaged water temperature, surface waters are warmed in the late afternoon for both 10m and 5m water depth (Figures 3a and 3b). The surface warming stops around 1700 and begins to cool around 1900. This pattern is consistent with Kaplan et al. (2003) in deeper water (h>12m). Kaplan et al. (2003) suggested that the combination of surface heat flux and cross-shore winds causes the surface water to accumulate with heat in the nearshore. Herdman et al. (2015) observed an almost identical behavior in water temperature (see Figure 4 in their paper) to Figure 3a and 3b, though their system was associated with a coastal lagoon. The water temperature in a lagoon warmed later in the day (2100), which was attributed to the combination of the CHF and the SHF creating the observed temporal lag in warming relative to just the SHF.

Assuming the SHF is similar at 5m and 10m, the heating (and cooling) contribution by the SHF can be removed by subtracting the upper 5m of the 10m water column from the 5m water column to compute a canonical temperature difference and is referred to as $\Delta T_{5m\text{-}10m}$. The same reasoning can be applied to removing the contribution of the AHF by assuming the AHF is the same at both 10m and 5m, as observed by Suanda et al. (2011). $\Delta T_{5m\text{-}10m}$ therefore represents the advective heat fluxes between 10m and 5m. $\Delta T_{5m\text{-}10m}$ is cooler from 2100 to 1100, suggesting that the T_{10m} is warmer than T_{5m} (Figure 3c). $\Delta T_{5m\text{-}10m}$ is larger as a function of depth. From 1300 to 1900 hours, $\Delta T_{5m\text{-}10m}$ is warmer at 5m than at 10m, with a maximum 0.5°C at 1600 (Figure 3c).

The canonical CHF_{10m} pattern indicates that there is typically an increase in the onshore heat transport across the 10m isobath that initiates at 0900, peaks at 1600, and decreases to a weak background onshore heat transport at 2100 (Figure 4). Meanwhile, the CHF_{5m} indicates that there is no flux (Figure 4). Because this is an hourly averaged estimate that is spatially averaged, and averaged over a canonical day, processes such as rip currents will not be resolved with this measure. In addition, similar to Hendrickson and MacMahan (2009), the semi-diurnal tide is averaged out over the canonical day, and can therefore be ignored. The inner shelf region shoreward of 10m should heat up shortly after the CHF develops (Figure 4) which is corroborated by the increase in water temperature observed at 5m (Figure 3c). The heating at 5m is therefore due, in part, to the cross-shore heat transport across the 10m isobath and the absence of transport at 5m. This is consistent with Kaplan et al. (2003) and Herdman et al. (2015) but described for a scaled-down estimate that occurs between two stations spaced 100m in the cross-shore between the 5m and 10m isobath.

The exact cross-shore location of where CHF goes zero between the 10m and 5m isobath cannot be resolved with only two moorings in the cross-shore. However, it is likely that it occurs near the 5m isobath since the temperature increases at 5m, and there is the maximum in $\Delta T_{5m\text{-}10m}$ and the CHF_{10m}. Since the 5m water depth represents the approximate edge of the surf zone, where different dynamical processes develop, further explaining why the CHF_{5m} tends to zero. Hally-Rosendahl et al. (2015) found that directly seaward of wave breaking, temperature stratification developed representing oceanic conditions.

The heating at 10m relative to 5m, when $\Delta T_{5m\text{-}10m}$ is negative, occurs when cross-shore wind forcing is minimal and the CHF at 10m is small. With the same reasoning as above, this suggests that the cross-shore location of where the CHF is zero is closer to the 10m isobath during this time. As the CHF at 10m reduces to near zero, the cross-shore warming contribution of the CHF moves offshore. At this point, the waters at 10m are warming at 2100 and become warmer than those at 5m (Figure 3c). Interestingly, the CHF lags the cross-shore wind stress by approximately 1 hr. It is believed that surface currents remain in motion owing to inertia. In addition, in the absence of a cross-shore wind stress due to the afternoon sea breeze and there is no significant land breeze in Monterey Bay, CA (Hendrickson and MacMahan 2009; Suanda et al. 2011), there is weak wave-forcing which would induce a seaward flow that is maximum near the surface. This may explain why the surface waters have minimal difference in temperature.

By definition, the cross-shore location of the zero CHF is the location where material will accumulate and represents a barrier. For temperature, this location describes the location of enhanced heating and appears to extend to the edge of the surf zone in the late afternoon and moves offshore in the evening. This is consistent with a surface intensified onshore flow driven by onshore winds over a stratified water column at the inner shelf (Fewings et al. 2008; Horowitz and Lentz 2014) by diurnal sea breeze (Hendrickson and MacMahan 2009). Note the focus of this effort is on the cross-shore transport, and assumes the alongshore transport is minimal (Suanda et al., 2011).

THIS PAGE INTENTIONALLY LEFT BLANK

V. CONCLUSION

The canonical water temperature response to diurnal sea breeze wind forcing and surface heating over the inner shelf off Del Monte beach in southern Monterey Bay is observed with co-located temperature and velocity profiles from two cross-shore arrays spanning between water depths of 5m and 10m for 45 days. A canonical day, based on local time, is chosen due to the strong influence of diurnal sea breeze wind forcing (Hendrickson and MacMahan 2009; Suanda et al. 2011). A ~1.5°C warming of surface waters in the late afternoon from 1200 to 1900 is attributed to a diurnal accumulation of heat due to onshore diurnal wind forcing, inducing a maximum CHF of $4\text{x}10^5$W/m at 1600, and surface heating; this scaled down version is consistent with the findings of Kaplan et al. (2003) in waters deeper than 12m and Herdman et al. (2015) in a shallow tropical lagoon. An observed increase in water temperature of 0.5°C at 5m relative to 10m from 1200 to 1700 indicates that the surface waters at the 5m mooring accumulate more heat than the 10m when wind forcing is onshore. This, along with an increase to $4\text{x}10^5$ W/m in the CHF_{10m} while the CHF_{5m} remained at zero, suggests that onshore winds drive an onshore transport of heat across the 10m isobath, which contributes, to a ~0.5°C heating at the 5m isobath relative to the 10m isobath. Although the exact location of zero CHF cannot be resolved in this study, the accumulation of heat at 5m suggests that the cross-shore location of zero CHF is near the 5m isobath. When cross-shore wind forcing becomes minimal in the evening and early morning from 2100 to 0800, the CHF at 10m decreases to near zero and the temperature of the water at 10m becomes ~0.3°C greater than the temperature at 5m, suggesting that the cross-shore location of zero CHF is closer to the 10m isobath during this time. The proposed diurnal cross-shore migration location of zero CHF implies that there is a diurnal migration of a barrier to cross shelf material transport between 10m and 5m over the inner shelf just outside of the surf zone as suggested by the canonical day, which does not include subtidal or wave breaking processes nor the alongshore heat flux.

THIS PAGE INTENTIONALLY LEFT BLANK

LIST OF REFERENCES

Austin, J. A., 1999, The role of the alongshore wind stress in the heat budget of the North Carolina inner shelf, *J. Geophys. Res.*, (C8), 18187–18203, doi.org/10.1029/1998JC900122.

Brown, J., J. MacMahan, A. Reniers, and E. Thornton, 2009, Surf zone diffusivity on a rip-channeled beach, *J.Geophys. Res.*, **114**(11), doi.org/10.1029/2008JC005158.

Brown, J. A., J. H. MacMahan, A. J. Reniers, and E. B. Thornton, 2015, Field observations of surf zone–inner shelf exchange on a rip-channeled beach, *J. Phys. Oceanogr.*, **45**, 2339–2355, doi.org/10.1175/JPO-D-14-0118.1.

Clark, D. B., S. Elgar, and B. Raubenheimer, 2012, Vorticity generation by short-crested wave breaking, *Geophysical Res. Letters*, **39**(24), doi.org/10.1029/2012GL054034.

Clark, D. B., L. Lenain, F. Feddersen, E. Boss, and R. T. Guza, 2014, Aerial imaging of fluorescent dye in the near shore, *J. Atmos. Oceanic Technol*., **31**, 1410–1421, doi.org/10.1175/JTECH-D-13-00230.1.

Clarke, L. B., D. Ackerman, and J. Largier, 2007, Dye dispersion in the surf zone: Measurements and simple models, *Continental Shelf Research*, **27**(5), 650–669, doi.org/10.1016/j.csr.2006.10.010.

Dever, E. P., and S. J. Lentz, 1994, Heat and salt balances over the northern California shelf in winter and spring, *J. Geophys. Res*., **99**(C8), 16001–16017, doi.org/10.1029/94JC01228.

Feddersen, F., 2014, The generation of surfzone eddies in a strong alongshore current, *J. Phys. Oceanogr*., **44**, 600–617, doi.org/10.1175/JPO-D-13-051.1.

Fewings, M. R., and S. J. Lentz, 2011, Summertime cooling of the shallow continental shelf, *J. Geophys. Res*., **116**, C07015, doi.org/10.1029/2010JC006744.

Fewings, M., S.J. Lentz, and J. Fredericks, 2008, Observations of cross-shelf flow driven by cross-shelf winds on the inner continental shelf, *J. Phys. Oceanogr*., **38**, 2358–2378, doi.org/10.1175/2008JPO3990.1.

Grant, S. B., J. H. Kim, B. H. Jones, S. A. Jenkins, J. Wasyl, and C. Cudaback, 2005, Surf zone entrainment, along-shore transport, and human health implications of pollution from tidal outlets, *J. Geophys. Res*., **110**, C10025, doi.org/10.1029/2004JC002401.

Hally-Rosendahl, K., F. Feddersen, D. B. Clark, and R. T. Guza, 2015, Surfzone to inner-shelf exchange estimated from dye tracer balances, *J. Geophys. Res. Oceans*, **120**, 6289–6308, doi.org/10.1002/2015JC010844.

Hendrickson, J., and J. MacMahan, 2009, Diurnal sea breeze effects on inner-shelf cross-shore exchange, *Continental Shelf Res*., **29**(18), 2195–2206, doi.org/10.1016/j.csr.2009.08.011.

Herdman, L. M. M., J. L. Hench, and S. G. Monismith, 2015, Heat balances and thermally driven lagoon-ocean exchanges on a tropical coral reef system (Moorea, French Polynesia), *J. Geophys. Res. Oceans*, **120**, 1233–1252, doi.org/10.1002/2014JC010145.

Horwitz, R. and S. J. Lentz, 2014, Inner-shelf response to cross-shelf wind stress: the importance of the cross-shelf density gradient in an idealized numerical model and field observations, *J. Phys. Oceanogr*., **44**, 86–103, doi.org/10.1175/JPO-D-13-075.1.

Kaplan, D. M., J. L. Largier, S. Navarrete, R. Guiñez, and J. C. Castilla, 2003, Large diurnal temperature fluctuations in the nearshore water column, *Estuarine, Coastal and Shelf Science*, **57**(3), 385–398, doi.org/10.1016/S0272-7714(02)00363-3.

Kumar, N. and F. Feddersen, 2017a, The effect of stokes drift and transient rip currents on the inner shelf. Part I: no stratification, *J. Phys. Oceanogr*., **47**, 227–241, doi.org/10.1175/JPO-D-16-0076.1.

Kumar, N. and F. Feddersen, 2017b, A new offshore transport mechanism for shoreline-released tracer induced by transient rip currents and stratification, *Geophys. Res. Lett*., **44**, 2843–2851, doi.org/10.1002/2017GL072611.

Lamas, L., A. Peliz, J. Dias, P. B. Oliveira, M. M. Angelico, J. J. Castro, J. N. Fernandes, A. Trindale, and T. Cruz, 2017, Diurnal variability of inner-shelf circulation in the lee of a cape under upwelling conditions, *Continental Shelf Res*., **143**, 67–77, doi.org/10.1016/j.csr.2017.06.006.

Large, W.G., and S. Pond, 1982, Sensible and latent heat flux measurements over the ocean, *J. Phys. Oceanogr*., **12**, 464–482, doi.org/10.1175/1520-0485(1982)012<0454:SALHFM>2.0.CO;2.

Lentz, S. J., 1987, A heat-budget for the northern California shelf during CODE-2, *Journal of Geophysical Res*., **92**(C13), doi.org/10.1029/JC092iC13p14491.

Lentz, S. J., and M. R. Fewings, 2012, The wind- and wave-driven inner-shelf circulation, *The Annual Review of Marine Science*, **4**, 317–343, https://doi.org/10.1146/annurev-marine-120709-142745.

Lentz, S.J., M. Fewings, P. Howd, J. Fredericks, and K. Hathaway, 2008, Observations and a model of undertow over the inner continental shelf, *J. Phys. Oceanogr*., **38**, 2341–2357, doi.org/10.1175/2008JPO3986.1

MacMahan, J. H., E. B. Thornton, and A. J. Reniers, 2006, Rip current review, *Coastal Engineering*, **53**(2-3), 191–208, doi.org/10.1016/j.coastaleng.2005.10.009.

MacMahan, J. H., E. B. Thornton, T. P. Stanton, and A. J. Reniers, 2005, RIPEX: Observations of a rip current system, *Marine Geology*, **218**(1-4), 113–134, doi.org/10.1016/j.margeo.2005.03.019.

Molina, L., G. Pawlak, J. R. Wells, S. G. Monismith, and M. A. Merrifield, 2014, Diurnal cross-shore thermal exchange on a tropical forereef, *Journal of Geophysical Res. Oceans*, **119**(9), 6101–6120, doi.org/10.1002/2013JC009621.

Noble, M., B. Jones, P. Hamilton, J. Xu, G. Robertson, L. Rosenfeld, and J. Largier, 2009, Cross-shelf transport into nearshore waters due to shoaling internal tides in San Pedro Bay, CA., *Continental Shelf Res*., **29**(15), doi.org/10.1016/j.csr.2009.04.008.

Orzech, M. D., E. B. Thornton, J. H. MacMahan, W. C. O'Reilly, and T. P. Stanton, 2010, Alongshore rip channel migration and sediment transport, *Marine Geology*, **271**(3-4), 278–291, doi.org/10.1016/j.margeo.2010.02.022.

Pineda, J., 1994, Internal tidal bores in the nearshore – warm-water fronts, seaward gravity currents and the onshore transport of Neustonic Larvae, *Journal of Marine Res*., **52**(3), doi.org/10.1357/0022240943077046.

Pawlowicz, R. B., S. Beardlsey, S. Lentz, E. Dever, and A. Anis, 2001, Software simplifies air-sea data estimates, *Eos Trans. AGU*, **82**(1), doi.org/10.1029/01EO00004.

Reniers, A. J. H. M., J. H. MacMahan, E. B. Thornton, T. P. Stanton, M. Henriquez, J. W. Brown, J. A. Brown, and E. Gallagher, 2009, Surf zone surface retention on a rip-channeled beach, *J. Geophys. Res*., **114**, doi.org/10.1029/2008JC005153.

Roth, M. K., J. MacMahan, A. Reniers, T. M. Ozgokmen, and K. Woodall, 2016, Observations of inner shelf cross-shore surface material transport adjacent to a coastal inlet in the northern Gulf of Mexico, *Continental Shelf Res*., **137**, 142–153, doi.org/10.1016/j.csr.2016.12.017.

Send, U., R. C. Beardsley, and C. D. Winant, 1987, Relaxation from upwelling in the coastal ocean dynamics experiment, *J. Geophys. Res*., **92**(C2), 1683–1698, doi.org/10.1029/JC092iC02p01683.

Spydell, M. S., 2016, The suppression of surfzone cross-shore mixing by alongshore currents, *Geophys. Res. Lett.*, **43**, 9781–9790, doi.org/10.1002/2016GL070626.

Spydell, M., F. Feddersen, R.T. Guza, and W.E. Schmidt, 2007, Observing surf-zone dispersion with drifters, *J. Phys. Oceanogr.*, **37**, 2920–2939, doi.org/10.1175/2007JPO3580.1.

Sinnett, G., and F. Feddersen, 2014, The surf zone heat budget: The effect of wave heating, *American Geophysical Union*, **40(**21), 7217–7226, doi.org/10.1002/2014GL061398.

Suanda, S. H., J. A. Barth, and C. B. Woodson, 2011, Diurnal heat balance for the northern Monterey Bay inner shelf, *J. Geophys. Res.*, **116**(C9), doi.org/10.1029/2010JC006894.

Tilburg, C. E., 2003, Across-shelf transport on a continental shelf: do across-shelf winds matter? *J. Phys. Oceanogr.*, **33**(12), 2675–2688, doi.org/10.1175/1520-0485(2003)033<2675:ATOACS>2.0.CO;2.

Walter, R. K., E. C. Reid, K. A. Davis, K. J. Armenta, K. Merhoff, and N. J. Nidzieko, 2017, Local diurnal wind-driven variability and upwelling in a small coastal embayment, *J. Geophys. Res. Oceans*, **122**(2), 955–972, doi.org/10.1002/2016JC012466.

Walter, R. K., C. B. Woodson, R. S. Arthur, O. B. Fringer, and S. G. Monismith, 2012, Nearshore internal bores and turbulent mixing in southern Monterey Bay, *J. Geophys. Res.*, **117**(C7), doi.org/10.1029/2012JC008115.

INITIAL DISTRIBUTION LIST

1. Defense Technical Information Center
   Ft. Belvoir, Virginia

2. Dudley Knox Library
   Naval Postgraduate School
   Monterey, California